Journal of Molecular Catalysis A: Chemical 296 (2008) 47–53

Contents lists available at ScienceDirect

Journal of Molecular Catalysis A: Chemical

journal homepage: www.elsevier.com/locate/molcata

TPD and TPSR study of CO interaction with $CuO–CeO_2$ catalysts

George Avgouropoulos, Theophilos Ioannides*

Foundation for Research and Technology-Hellas, Institute of Chemical Engineering and High Temperature Chemical Processes (FORTH/ICE-HT), Stadiou str., PO Box 1414, GR-26504, Patras, Greece

ARTICLE INFO

Article history:
Received 1 August 2008
Received in revised form 5 September 2008
Accepted 8 September 2008
Available online 20 September 2008

Keywords:
CO
Adsorption
TPD
Ceria
Copper oxide

ABSTRACT

The interaction of CO and CO_2 with $CuO–CeO_2$ catalysts, prepared by a citrate-hydrothermal method, has been studied employing the techniques of temperature-programmed desorption (TPD) and temperature-programmed surface reaction (TPSR) of preadsorbed CO, as well as TPD of preadsorbed CO_2. The effect of copper content and activation temperature on the adsorptive behavior of the catalysts has been investigated. TPD studies of preadsorbed CO showed that a small fraction of CO is reversibly adsorbed, while most of it undergoes reaction with surface oxygen and desorbs as CO_2. Such profiles of CO_2 consist of a peak at 100–120 °C along with CO_2 desorption at high temperatures, which was significant for catalysts activated at 300 °C. TPSR of preadsorbed CO showed that reversibly adsorbed CO is highly reactive in the presence of gaseous oxygen. Catalytic sites, which form carbonates during interaction with CO, get eliminated with increase of catalyst activation temperature and do not contribute to the steady-state activity of the catalysts. The effect of CeO_2 appears to be mainly related to stabilization of highly dispersed copper oxide species and to creation of additional sites for CO adsorption and reaction, probably at the interface between the two oxides.

1. Introduction

The $CuO–CeO_2$ catalytic system has been studied by a large number of investigators in view of its application in (preferential) CO oxidation and many techniques have been employed for its characterization [1–34]. These include N_2O chemisorption, TPR, SEM, TEM, XRD, XPS, EXAFS, EPR and FTIR spectroscopy. On the other hand, temperature-programmed techniques, such as temperature-programmed desorption (TPD) and temperature-programmed surface reaction (TPSR), have been less often used to study the characteristics of CO adsorption on $CuO–CeO_2$. CO-TPD experiments over $CuO–CeO_2$ catalysts with CuO content up to 15 wt.% prepared by impregnation have been carried out by Luo et al. [14]. They found that almost no CO is desorbing from the catalysts and the TPD profile consists of a single CO_2 peak at 110 °C. Martinez-Arias et al. [4] have carried out CO-TPD for a 1 wt.% CuO/CeO_2 catalyst prepared by impregnation and activated at 500 °C. The reported TPD profiles consist of a small CO peak at 70–80 °C and a CO_2 peak at 110 °C with a tail extending up to 450 °C. Similar desorption behavior has been reported recently by Caputo et al. [33] during CO-TPD over a 4 wt.% CuO/CeO_2 catalyst prepared by impregnation. We have also reported on the adsorption and reaction of CO on combustion-synthesized $CuO–CeO_2$ catalysts [32]. Adsorption of CO was found to proceed through initial reduction of Cu^{2+} and formation of carbonate species followed by adsorption of CO on reduced Cu^{+} sites.

In the present work, we examine the interaction of CO with $CuO–CeO_2$ materials, prepared via a citrate-hydrothermal method, employing the techniques of TPD and TPSR of preadsorbed CO. TPD experiments of preadsorbed CO_2 were also carried out, as CO_2 is the reaction product between CO and O_2. The effect of copper content and activation temperature on the adsorptive behavior of the catalysts has been investigated. Physicochemical characterization and activity data in preferential CO oxidation of these catalysts have been reported in a previous publication [1].

2. Experimental

2.1. Preparation of catalysts

$CuO–CeO_2$ samples were prepared via a citrate-hydrothermal method [1]. Aqueous solutions of metal acetates – cerium acetate [$Ce(C_2H_3O_2)_3{\cdot}1.5H_2O$] and copper acetate [$Cu(C_2H_3O_2)_2{\cdot}H_2O$] – were mixed with an aqueous solution of citric acid under continuous stirring. The molar ratios of citric acid to each metal acetate were adjusted as citric acid/Ce = 1/1 and citric acid/Cu = 2/3. The mixed solution was treated hydrothermally in a stainless steel autoclave, at 150 °C (heating rate = 2 °C min^{-1}) for 24 h. Following

* Corresponding author.
E-mail address: theo@iceht.forth.gr (T. Ioannides).

1381-1169/$ – see front matter © 2008 Elsevier B.V. All rights reserved.
doi:10.1016/j.molcata.2008.09.013

hydrothermal treatment, the autoclave was opened, excess water was decanted and the remaining paste was dried for 12 h at 120 °C and subsequently activated at 300, 400 or 500 °C under a flowing 20% O_2/He mixture (20 cm^3 min^{-1}) for 2 h.

For comparison purposes, two additional catalysts, namely 7.5 wt.% CuO/CeO_2 and 7.5 wt.% CuO/Al_2O_3, were prepared by impregnation using an aqueous $Cu(NO_3)_2{\cdot}3H_2O$ solution of the desired concentration. The supports in this case were CeO_2 made via the hydrothermal-citrate method (S_{BET} = 27.6 m^2 g^{-1}) and commercial Al_2O_3 (Alfa-Aesar, S_{BET} = 90 m^2 g^{-1}). The samples were dried overnight in an oven at 120 °C and then activated at 400 °C under a flowing 20% O_2/He mixture (20 cm^3 min^{-1}) for 2 h.

All samples were sieved to obtain the desired fraction of particle diameter between 90 and 180 μm. For ease of reference, the catalysts are encoded as follows: *x*Cu-TTT, where *x* is the Cu/(Cu + Ce) atomic ratio and TTT is the activation temperature. For example, the catalyst 0.25Cu-400 was prepared at a ratio of Cu/(Cu + Ce) = 0.25 and was activated at 400 °C.

2.2. Temperature-programmed techniques (CO-TPD, CO_2-TPD and TPSR)

TPD and TPSR experiments were performed in a fixed-bed reactor system, described in detail elsewhere [5]. Prior to TPD, the catalyst (30–50 mg with particle size 90 μm < d_p < 180 μm) was treated at its activation temperature for 30 min under a 20% O_2/He flow (20 cm^3 min^{-1}), and cooled under the same gas flow to 32 °C. After purging with He, adsorption of CO (CO-TPD and TPSR) or CO_2 (CO_2-TPD) was carried out under a flow of 1% CO/He or 1.7% CO_2/He mixture, respectively. Following completion of the adsorption, as indicated by stable signals of CO or CO_2 in the mass spectrometer, the reactor was purged with pure He for ~10 min. Then, the TPD or TPSR run was started under a flow of 40 cm^3 min^{-1} of He (CO-TPD and CO_2-TPD) or 1% O_2/He (TPSR-O_2) with a heating rate of 20 °C min^{-1} up to the corresponding activation temperature for each catalyst. This was followed by soak at this temperature until the MS signals returned to baseline levels. A mass spectrometer (Omnistar/Pfeiffer Vacuum) was used for on-line monitoring of effluent gases. Mass peaks of CO, CO_2, O_2, H_2 and H_2O were monitored during the experiments. The only products detected, in all cases, were CO and CO_2. CO (*m*/*z* 28) and CO_2 (*m*/*z* 44) signals were calibrated using gas mixtures prepared in situ and analyzed in a pre-calibrated gas chromatograph with a TC detector (Shimadzu 14B). The contribution of CO_2 to the *m*/*z* 28 signal was taken into account for the calculation of CO concentration.

3. Results

3.1. TPD of CO and CO_2

As stated in Section 2, the maximum temperature during TPD was the same as the corresponding activation temperature of the catalyst tested in the specific run. In the case of catalysts activated at 300 °C, for example, the TPD run consisted of a ramp of 20 °C min^{-1} to 300 °C, followed by soak at this temperature, until the signals returned to baseline levels. Typical TPD profiles along with the applied temperature program after CO adsorption at RT are shown in Fig. 1(a) and (b) for 0.50Cu–300 and 0.50Cu–400 catalysts, respectively. The majority of adsorbed CO desorbs as CO_2, but there is also molecular desorption of CO at low temperatures with a peak at 75 °C. CO desorption starts immediately upon initiation of the temperature ramp. The CO_2 profiles are characterized by a main peak at ~110 °C and a second peak above 300 °C, which is more intense for the 0.50Cu-300 sample.

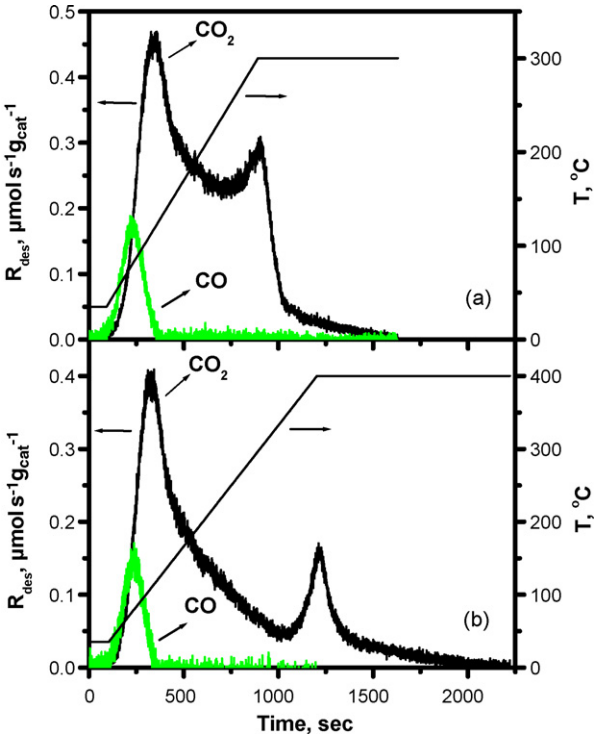

Fig. 1. CO and CO_2 TPD profiles along with the applied temperature program after CO adsorption at RT on 0.50Cu catalyst, activated at 300 °C (a) and 400 °C (b).

The effect of catalyst Cu content on the resulting TPD profiles of CO_2 following CO adsorption is depicted in Fig. 2(a)–(c) for catalysts activated at 300, 400 and 500 °C, respectively. The corresponding profiles of CuO and CeO_2 are also shown for comparison purposes. CO desorption profiles were similar in all cases to those shown in Fig. 1 and are not plotted for reasons of clarity. In the case of CeO_2, very small amounts of CO_2 and no CO were detected during TPD, with CO_2 appearing above 225 °C and slightly increasing with temperature. The CO_2 profile of pure CuO consisted of a small peak at ~100 °C with a tail extending up to 300 °C. Regarding CuO–CeO_2 catalysts, the profiles of 0.25Cu, 0.50Cu and 0.75Cu bear many similarities, while the behavior of 0.10Cu is significantly different: CO_2 desorption from the 0.10Cu-300 sample starts above 130 °C giving a broad peak at 200–250 °C compared to a peak at 120 °C for all other catalysts activated at 300 °C (Fig. 2(a)). The CO_2 profiles of catalysts activated at 400 °C (Fig. 2(b)) also indicate a gradual shift of the CO_2 peak to lower temperatures accompanied by an increase in the amount of desorbed CO_2 with increase of Cu content. When the activation temperature is 500 °C (Fig. 2(c)), the high-temperature CO_2 peak has diminished and the profiles are characterized by a peak at 100 °C (150 °C for 0.10Cu). Increase of catalyst activation temperature leads to a decrease of the amount of CO_2 desorbing from the catalysts. The high-temperature (HT) CO_2 desorption peak diminishes with increase of catalyst activation temperature: it is quite significant for the samples activated at 300 °C, but has essentially disappeared for catalysts activated at 500 °C. In addition, the intensity of the low-temperature (LT) CO_2 peak decreases by half. A small shift of the CO_2 peak temperature from 110–120 to 100 °C is also observed with increase of the catalyst activation temperature.

The quantities of desorbed CO_2 and CO (in μmol g^{-1}) and the specific adsorption capacity (in μmol m^{-2}) of the catalysts following adsorption of CO at RT are presented in Table 1 (calculation of specific adsorption capacities employed the specific surface areas, S_{BET}, of all catalysts, which are given in Table 2). The quantity of desorbed CO is 5–15% of the total (CO + CO_2) amount desorbed from

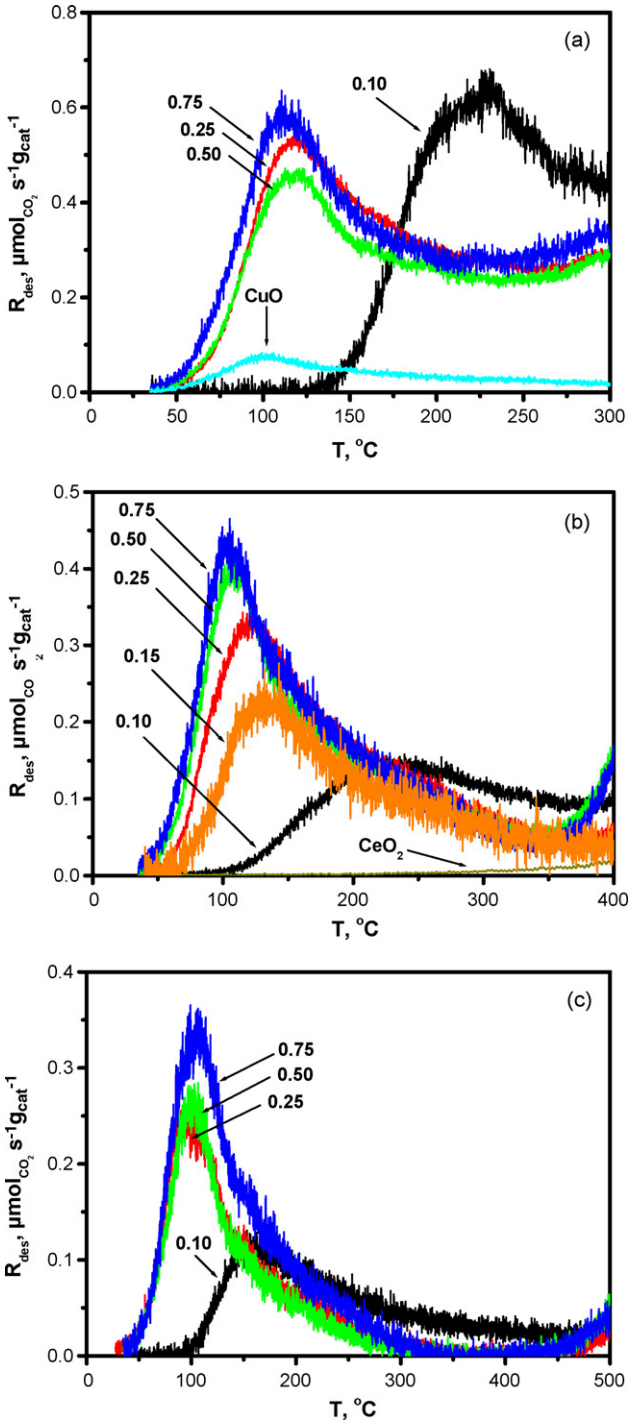

Fig. 2. Effect of copper content on TPD profiles of CO_2, after adsorption of CO at RT, for CuO–CeO_2 catalysts activated at (a) 300 °C, (b) 400 °C and (c) 500 °C.

the catalysts and there appears no definite trend with Cu content or activation temperature. The quantity of desorbed CO_2 is up to one order of magnitude higher in Cu–Ce catalysts compared to pure CuO and increases with increase of Cu content of the catalysts. On the other hand, the quantity of desorbed CO_2 decreases by 3–4 times with increase of catalyst activation temperature from 300 to 500 °C. The specific adsorption capacity of Cu–Ce catalysts is larger than the one of pure CuO and pure CeO_2 and it tends to increase with: (i) increase of copper loading and (ii) decrease of activation temperature. The CuO/CeO_2 catalyst prepared by impregnation has similar specific adsorption capacity to the 0.15Cu catalyst, while the CuO/Al_2O_3 sample shows the lowest capacity among all catalysts. By comparison, the quantity of desorbed CO_2 and CO for a 0.15Cu catalyst, prepared by combustion, was 131.2 μmol g^{-1} [32] and its corresponding specific capacity is 3.36 μmol m^{-2}. These values are quite similar to the ones presented in Table 1 for catalysts prepared by the citrate method.

TPD experiments following adsorption of CO_2 at RT were also carried out. Adsorption of CO_2 is interesting from the fact that CO_2 acts as an inhibitor of CO oxidation [1,5,6,15]. The TPD profiles of CO_2 after its adsorption at RT are shown in Fig. 3 for CuO–CeO_2 catalysts, as well as for pure CuO and CeO_2. In the case of pure CuO, CO_2 desorption took place in the form of a peak at 100 °C with a tail up to 300 °C. For pure CeO_2, the CO_2 profile consisted of a LT main peak at 85 °C and a second – lower in intensity – peak at 250 °C. In the case of CuO–CeO_2 catalysts, a main CO_2 peak at 90 °C was found with a tail up to 300–400 °C. The high-temperature CO_2 desorption is most significant at low-copper loadings (0.10Cu) and gradually weakens with increase of copper loading. The desorbed quantity of CO_2 expressed in μmol g^{-1} and the specific CO_2 adsorption capacity of the catalysts (μmol m^{-2}) are presented in Table 3. Similarly to the case of CO adsorption, the specific CO_2 adsorption capacity decreases with increase of catalyst activation temperature. On the other hand, the specific capacity of CuO–CeO_2 catalysts attains intermediate values between those for pure CuO and pure CeO_2. Hence, it is quite probable that CO_2 adsorption on CuO–CeO_2 catalysts takes place on both CuO and CeO_2 moieties. In addition, the amounts of adsorbed CO_2 are considerably smaller than the amounts of adsorbed CO, as deduced from comparison of the results in Tables 1 and 3. The relative amounts of CO_{ads}/CO_{2ads} appear also to increase with increase of T_{act}.

3.2. TPSR of adsorbed CO with O_2

In TPSR experiments, the temperature ramp following adsorption of CO at RT was carried out using an O_2/He mixture as the carrier gas. No CO was found to desorb in this case, in contrast to what was found during TPD. Therefore, reversibly adsorbed CO gets oxidized in the presence of gas phase oxygen. The only product detected in the gas phase was CO_2 and the corresponding TPSR profiles of CO_2 from 0.25Cu catalysts activated at 300, 400 and 500 °C are shown in Fig. 4. It can be observed that the reactivity of preadsorbed CO increases with increase of activation temperature from 300 to 400 °C, as indicated from the shift of peak temperature from 120 to 70 °C. Further increase of T_{act} from 400 to 500 °C leads to decrease of the amount of desorbed CO_2 (as in the case of TPD of preadsorbed CO), but the shapes of both profiles are similar in all respects. The TPSR profiles of CO_2 from CuO–CeO_2 catalysts of varying Cu content activated at 400 °C, as well as of pure CuO, are shown in Fig. 5. Compared to TPD, the peak temperatures of CO_2 over CuO–CeO_2 catalysts are shifted to lower temperatures in the presence of gas phase O_2. In the case of 0.10Cu, for example, the observed shift is from 220 to 120 °C, while for 0.50Cu the corresponding shift is from 110 to 70 °C. In contrast, there is no appreciable shift in the case of pure CuO. All profiles are rather broad showing a tail extending up to 400 °C. In order to be able to compare more clearly the effect of gas phase O_2 on the reactivity of adsorbed CO, the TPD and TPSR profiles from the 0.15Cu–400, 7.5 wt.% CuO/CeO_2 and 7.5 wt.% CuO/Al_2O_3 catalysts are compared in Figs. 6(a)–(c), respectively. It can be observed that the CO_2 profile during TPSR is essentially the sum of CO and CO_2 TPD profiles, i.e. species, which desorb as CO in the absence of oxygen, appear as CO_2 in the presence of oxygen. There is not any significant difference in the shape and position of TPSR profiles of 0.15Cu-400, 7.5 wt.% CuO/CeO_2 and 7.5 wt.% CuO/Al_2O_3 catalysts, but only in the

Table 1
Amounts (expressed as μmol g^{-1} and μmol m^{-2}) of CO_2 and CO desorbed in CO-TPD experiments.

Catalyst	Desorbed amounts of CO and CO_2								
	μmol g^{-1}						μmol $(CO+CO_2)$ m^{-2}		
	T_{act} = 300 °C		T_{act} = 400 °C		T_{act} = 500 °C		T_{act} = 300 °C	T_{act} = 400 °C	T_{act} = 500 °C
	CO_2	CO	CO_2	CO	CO_2	CO			
CeO_2			7.5	0.0				0.27	
0.10Cu	284.6	16.5	108.5	11.2	72.5	13.1	3.54	1.85	1.91
0.15Cu			129.5	22.4				2.39	
0.25Cu	286.6	33.3	161.8	20.4	85.2	14.7	3.79	2.75	2.12
0.50Cu	249.8	21.0	201.5	18.9	94.9	13.8	3.98	4.36	3.32
0.75Cu	295.9	39.0	205.4	21.0	107.6	19.5	5.47	4.49	4.18
CuO	31.4	2.2					1.58		
7.5 wt.% CuO/CeO_2			52.9	9.4				2.66	
7.5 wt.% CuO/Al_2O_3			10.6	4.0				0.17	

Table 2
Specific surface areas, S_{BET}, of catalysts activated at various temperatures [1].

Catalyst	S_{BET} (m^2 g^{-1})		
	T_{act} = 300 °C	T_{act} = 400 °C	T_{act} = 500 °C
0.10Cu	85.1	64.8	44.8
0.15Cu	86.4	63.5	41.9
0.25Cu	84.3	66.3	47.1
0.50Cu	68.1	50.5	32.7
0.75Cu	61.2	50.4	30.4
CuO	21.3		
7.5 wt.% CuO/CeO_2		23.4	
7.5 wt.% CuO/Al_2O_3		88.1	

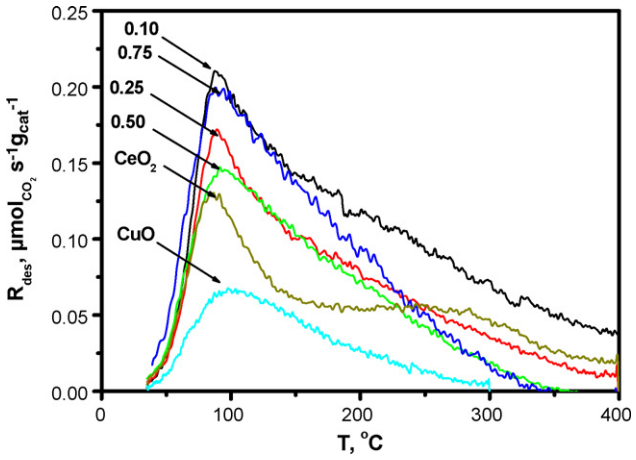

Fig. 3. TPD profiles of CO_2 after CO_2 adsorption at RT, for Cu-400 catalysts and pure CuO and CeO_2 samples.

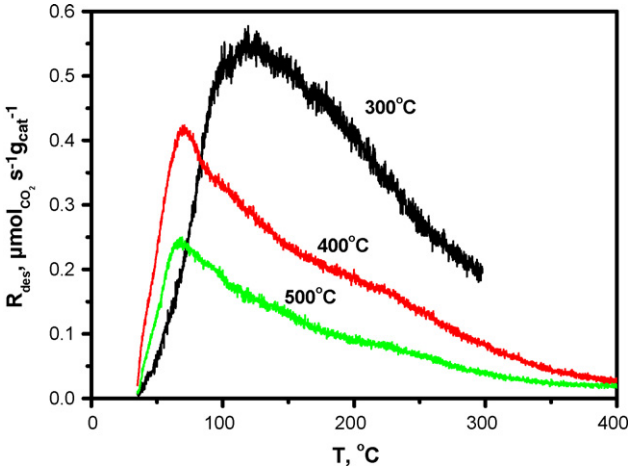

Fig. 4. TPSR profiles of CO_2 (carrier gas: 1% O_2/He) after adsorption of CO at RT, for 0.25Cu catalyst activated at 300, 400 and 500 °C.

amount of produced CO_2, which is considerably smaller over the alumina-supported catalyst. The amounts of CO_2 produced during TPSR were, in all cases, almost equal to the sum of $(CO+CO_2)$ produced during TPD of preadsorbed CO. This result, therefore, helps validate and confirm the corresponding TPD results.

4. Discussion

The observation of molecular desorption of CO during TPD implies that part of CO adsorbs reversibly on all catalysts when the adsorption is carried out at RT. This is in line to what has been found previously by us [32], as well as other investigators [4]. Reversibly adsorbed CO is obviously bound on a reduced Cu^{1+} site, which has been created during exposure of the catalysts to CO prior to TPD or TPSR. FTIR studies of adsorbed CO over CuO–CeO_2 indicate

Table 3
Amounts (expressed as μmol g^{-1} and μmol m^{-2}) of CO_2 desorbed in CO_2-TPD experiments.

Catalyst	Desorbed amounts of CO_2					
	μmol CO_2 g^{-1}			μmol CO_2 m^{-2}		
	T_{act} = 300 °C	T_{act} = 400 °C	T_{act} = 500 °C	T_{act} = 300 °C	T_{act} = 400 °C	T_{act} = 500 °C
CeO_2		61.6			2.23	
0.10Cu		115.8			1.79	
0.25Cu	144.3	73.7	29.8	1.71	1.11	0.63
0.50Cu	113.2	62.4	32.4	1.66	1.24	0.99
0.75Cu	130.9	81.3	26.6	2.14	1.61	0.88
CuO	26.7			1.25		
7.5 wt.% CuO/CeO_2		28.6			1.22	

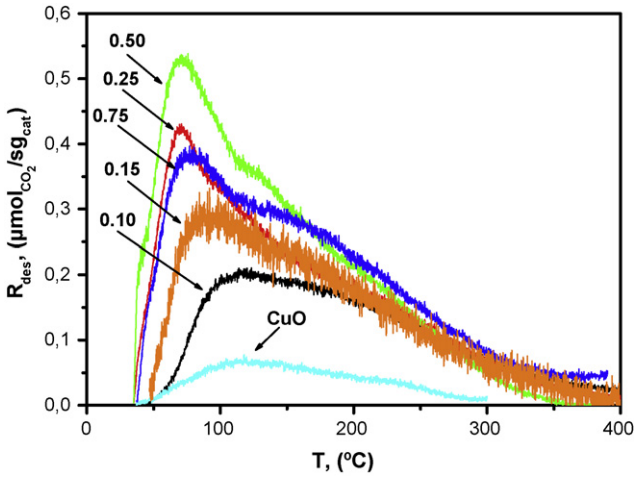

Fig. 5. TPSR profiles of CO_2 (carrier gas: 1% O_2/He) after adsorption of CO at RT, for Cu-400 catalysts and pure CuO.

formation of Cu^+ carbonyls due to interaction of CO with Cu^{2+} ions with unsaturated coordination leading to their reduction with accompanying CO_2 formation, while subsequent CO adsorption on reduced centers produces the Cu^+-carbonyl species [24]. Microcalorimetric studies of CO interaction with CuO–ZnO catalysts in the oxidized state have shown the occurrence of surface reduction by CO as indicated by the high heat of interaction, while the heat of adsorption of CO on the resulting Cu^+ centers takes values in the range of 110–66 kJ mol^{-1} [35]. Our TPD and TPSR results are in agreement with such a scheme of CO adsorption. The Cu^+–CO species are very reactive in the presence of gaseous oxygen, which is rapidly taken up by the reduced catalyst surface even at room temperature, as has been found by Caputo et al. [33]. Regarding CO_2 adsorption, CO_2-TPD experiments showed that CO_2 desorption takes place with peak at around 100 °C. It is expected, therefore, that the surface coverage of CO_2 will become quite low at temperatures around 150 °C or higher. This is in line with the observed inhibition effect of CO_2 during CO oxidation under steady-state conditions [1]. The observation that CO_2 inhibition is stronger over pure CuO than on CuO–CeO_2 catalysts may be attributed to: (i) the stronger adsorption of CO_2 on pure CuO compared to CuO–CeO_2 catalysts, as indicated by the higher CO_2 peak temperature in the former case and (ii) the higher value of the ratio CO_{ads}/CO_{2ads} on CuO–CeO_2 catalysts compared to pure CuO, indicating that CO_2 occupies a larger fraction of active sites on pure CuO, causing in this way a stronger inhibition.

4.1. Effect of Cu content on CO-TPD

In the case of pure CeO_2, CO_2 started to form above 225 °C and its formation rate increased gradually with temperature, but the amount of CO_2 produced was very low compared to CuO–CeO_2 catalysts. This result shows, however, that these small amounts of CO are held quite strongly on the CeO_2 surface, probably via formation of carbonate species. The total amount of ($CO + CO_2$), which is produced during TPD from CuO–CeO_2 catalysts does not increase in an analogous fashion with increase of Cu content. When the catalyst activation temperature is 300 °C, the total amount of ($CO + CO_2$) is in the range of 270–335 μmol g^{-1}. At the activation temperature of 400 °C, increase of Cu content from 0.10 to 0.75 leads to doubling of desorbed amount from 120 to ~230 μmol g^{-1}, while at T_{act} = 500 °C the corresponding increase is ~50%, i.e. from 85 to 127 μmol g^{-1}. This means that most of the added copper oxide does not contribute appreciably to the creation of sites for CO adsorption. Caputo et al. [33] have measured the quantity of adsorbed CO over a 4 wt.% CuO/CeO_2 catalyst to be 163 μmol g^{-1} corresponding to a specific capacity of 3.26 μmol m^{-2}. Jung et al. [34] have measured the irreversible CO uptake of a CuO–CeO_2 (5.1 wt.% Cu) catalyst at RT with a static method. They found a value of ~446 μmol g^{-1} for the catalyst activated at 500 °C (S_{BET} = 78 m^2 g^{-1}) and a value of ~125 μmol g^{-1} for the catalyst activated at 700 °C (S_{BET} = 22 m^2 g^{-1}), which was the most active one. It should be noted that these measurements were obtained with higher CO pressure (500 mm Hg) than that of the present work.

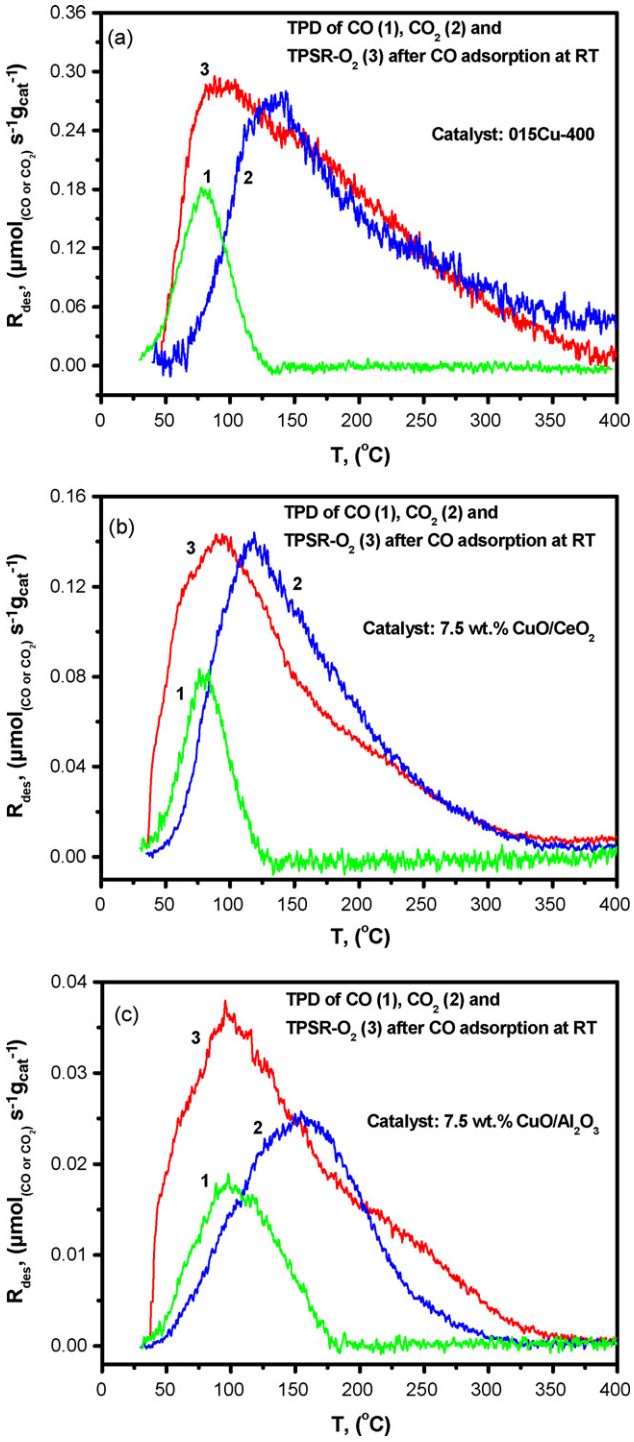

Fig. 6. TPD profiles of CO (1) and CO_2 (2) along with TPSR profiles of CO_2 (3) (carrier gas: 1% O_2/He) after adsorption of CO at RT on (a) 0.25Cu-400, (b) 7.5 wt.% CuO/CeO_2 and (c) 7.5 wt.% CuO/Al_2O_3 catalysts.

Table 4
Adsorption, Q/Q_{CuO}, and activity, R/R_{CuO}, ratios for CO adsorption and CO oxidation, respectively, over CuO–CeO_2 catalysts activated at various temperatures.

Catalyst	Q/Q_{CuO} [a]			R/R_{CuO} [b]		
	T_{act} = 300 °C	T_{act} = 400 °C	T_{act} = 500 °C	T_{act} = 300 °C	T_{act} = 400 °C	T_{act} = 500 °C
0.10Cu	183	73	52	54	73	57
0.15Cu	nm	60	nm	54	80	71
0.25Cu	71	41	22	40	57	38
0.50Cu	26	21	10	20	14	12
0.75Cu	17	12	6.5	6	3.6	2.8
7.5 wt.% CuO/CeO_2		25			36	
7.5 wt.% CuO/Al_2O_3		6			1.6	

[a] Q_{CuO} = 33.6 μmol g^{-1} (total desorbed CO + CO_2, Table 1).
[b] CO oxidation rates measured at 75 °C. Feed: 1% CO, 1.25% O_2, 50% H_2, He balance. W/F = 0.03 g s cm^{-3}; R_{CuO} = 0.25 μmol g^{-1} s^{-1} [1].

TPD profiles in Fig. 2 show that the CO_2 peak temperatures shift to lower values with increase of copper content, while the 0.10Cu catalyst shows a significant delay in the appearance of CO_2 in the gas phase compared to the other catalysts. When this catalyst was activated at 300 °C, the total amounts of CO and CO_2 desorbed after CO adsorption were ~300 μmol g^{-1}. The CuO loading of this catalyst is 615 μmol g^{-1} and the corresponding CO/Cu ratio is 0.5. This result indicates the presence of highly dispersed, isolated Cu^{2+} species on the surface. Increase of activation temperature to 400 or 500 °C causes a marked decrease in the amount of desorbed CO and CO_2 by 3–4 times to 120 and 85 μmol g^{-1}, respectively, implying a loss of adsorption sites due to agglomeration of copper ions with formation of very small CuO clusters. At the same time, TPD profiles showed a shift of CO_2 desorption to lower temperatures – hence easier decomposition of formed carbonates – with increase of T_{act}. Under steady-state CO oxidation conditions, the 0.10Cu catalyst had slightly higher activity when activated at 400 or 500 °C than at 300 °C [1], showing that the "lost" adsorption sites do not actually contribute to the catalyst activity. The same applies for the catalysts with Cu content of 0.15 and 0.25.

4.2. Effect of activation temperature of catalysts on CO-TPD

Significant amounts of CO_2 desorbing at high temperature were found over the catalysts activated at 300 °C. These were considerably diminished for catalysts activated at 400 °C and had almost disappeared, when T_{act} was 500 °C. A similar feature in CO-TPD over CuO–CeO_2 catalysts prepared by co-precipitation has been reported by Zou et al. [36] and may be attributed to decomposition of carbonate species formed upon reaction of adsorbed CO with surface oxygen. This explanation assumes that carbon dioxide formed on the surface is bound in a different mode compared to carbon dioxide adsorbed from the gas phase, because no high-temperature CO_2 peak was observed during CO_2-TPD. The main difference between CO_2 formed on the surface by reaction of adsorbed CO with surface oxygen and CO_2 adsorbed from the gas phase is that the former resides on a locally reduced surface due to abstraction of lattice oxygen. Formation of carbonates, carboxylates and linear adsorbed CO with exposure of CeO_2 to CO at room temperature has been previously reported [37,38]. Hilaire et al. [39] have also found that carbonate species are formed upon exposure of a Pd/CeO_2 catalyst to CO at 400 °C. These carbonate species were found to be quite stable on a reduced ceria surface, but decomposed with exposure in oxygen. Karpenco et al. [40] have also reported fast decomposition of carbonate species during oxidative treatment (O_2/N_2) at 180 °C of Au/CeO_2 catalysts. These carbonate species are generally associated with reduced sites (Ce^{3+}) and the oxidative treatment causes their decomposition with simultaneous oxidation of the ceria surface ($Ce^{3+} \rightarrow Ce^{4+}$). Comparison of TPD and TPSR profiles for the catalysts activated at 400 °C shows that CO_2 desorption is completed earlier during TPSR, as the CO_2 peak observed at 400 °C during TPD is absent in TPSR. This is in line with a greater instability of carbonates (thus larger tendency towards decomposition) in the presence of O_2.

It should be pointed out that the disappearance of the high-temperature CO_2 peak with increase of catalyst activation temperature has almost no effect on catalyst activity, because catalysts activated at 500 °C – for which this peak is not present – have comparable activities with catalysts activated at 300 °C [32]. CuO–CeO_2 catalysts exhibit activity in CO oxidation even at 50 °C, whereas at this temperature the species responsible for the HT CO_2 desorption will certainly be spectator species.

The low-temperature peak of CO_2 observed during TPD of preadsorbed CO was found to decrease by ~50% with increase of T_{act} from 300 to 500 °C, i.e. in an analogous fashion to the concomitant decrease of the surface area of the catalysts. Therefore, as far as the LT CO_2 peak is concerned, no significant change in the amount of the corresponding adsorbed CO per unit surface area of the catalyst takes place. The overall decrease in the amount of adsorbed CO per m^2 of catalyst with increase in T_{act} is due to the disappearance of the HT CO_2 peak. The shift of the CO_2 peak temperature from 120 to 100 °C with increase of T_{act} can be considered as an indication of enhancement of catalyst reactivity, because surface carbonates are less stable and tend to decompose at lower temperatures.

4.3. Adsorption sites and catalytic activity

Quantitative analysis of TPD and TPSR experiments has provided an estimation of the active sites of CuO–CeO_2 catalysts, i.e. of sites which are able to interact with CO at room temperature. The results of this analysis and the derived conclusions may be summarized as follows:

- Interaction of CO with all catalysts has identical features: (i) reactive adsorption leading to surface reduction and bound carbonates and (ii) adsorption of CO on reduced sites: this adsorption is weak and reversible. This type of adsorbed CO is highly reactive towards gaseous oxygen.
- Highly dispersed Cu^{2+} species (essentially isolated Cu^{2+}) which are more abundant on CuO–CeO_2 catalysts activated at low temperature, which possess a high surface area, get reduced by interaction with CO and form surface carbonates.
- Increase of catalyst activation temperature leads to CuO cluster growth and diminishes the HT CO_2 desorption feature.

The CO adsorption capacity and the catalytic activity in CO oxidation of all catalysts, is compared in Table 4, which depicts the adsorption ratio, Q/Q_{CuO} (Q is the sum of (CO + CO_2) desorbed during TPD expressed in μmol g^{-1}_{CuO} and Q_{CuO} is the corresponding value for pure CuO) and the activity ratio, R/R_{CuO} (R is the CO oxidation rate expressed in μmol s^{-1} g^{-1}_{CuO} and R_{CuO} the corresponding reaction rate for pure CuO). As the adsorption ratio, Q/Q_{CuO}, compares the

amount of CO adsorbed on the catalysts to that on pure CuO based on the same CuO mass, it provides an indication of the effect of the support (CeO_2 or Al_2O_3) on enhancing CuO dispersion and creating additional adsorption sites. The activity ratio, R/R_{CuO}, operates in an analogous fashion regarding catalytic activity. For example, 1 g of CuO contained in the 0.10Cu-300 catalyst adsorbs 183 times more CO and is 54 times more active in CO oxidation than pure CuO. The results of Table 4 show that the adsorption ratio decreases both with increase of copper content and with increase of activation temperature. This corresponds to a decrease of CuO dispersion due to diminishing of atomically dispersed copper ions and CuO cluster growth. The 7.5 wt.% CuO/CeO_2 catalyst, prepared by impregnation, has a smaller adsorption and activity ratio than the corresponding 0.15Cu–400 catalyst of the same CuO content, obviously due to its smaller surface area and the different preparation method. The 7.5 wt.% CuO/Al_2O_3 catalyst has the smallest adsorption ratio among all catalysts. The activity ratio decreases with increase of copper content in a fashion analogous to the adsorption ratio, but decreases with increase of activation temperature only for catalysts with high copper content (0.50Cu and 0.75Cu). In the case of catalysts with low copper content (0.10Cu–0.25Cu), the activity ratio shows a weak maximum at the activation temperature of 400 °C. A similar example can be derived from the work of Jung et al. [34], in which it is shown that the catalytic activities of a 5.1 wt.% $CuO–CeO_2$ catalyst prepared by co-precipitation and calcined at 500 °C or 900 °C are comparable, despite the fact that the surface area is more than 6 times lower and the CO uptake 14 times lower for the catalyst calcined at 900 °C. The observed trends of adsorption and activity ratios for our catalysts lead to the conclusion that the "lost" adsorption sites do not contribute to catalyst activity. On the basis of TPD results, these sites are most probably blocked by carbonate species under steady-state reaction conditions. DRIFTS experiments under PROX reaction conditions have shown the formation of different carbonate species on $CuO–CeO_2$ catalysts, located at the interfacial region of the support in contact with the dispersed copper oxide species [18]. Another interesting observation regarding the data in Table 4 is that the values of the adsorption and activity ratios for most catalysts are quite similar (exceptions are the 0.10Cu-300 and 0.75Cu). This implies that the enhanced CO oxidation activity of $CuO–CeO_2$ catalysts compared to CuO is in a major part due to their higher active site density and not to a higher intrinsic site activity. If one calculates the Q/Q_{CuO} ratio on a surface area basis, it turns out that it obtains values in the range of 1.2–3.5, hence $CuO–CeO_2$ catalysts have a density of sites for CO adsorption 1.2–3.5 times higher than the one of pure CuO. These additional sites for CO adsorption and reaction reside probably at the interface between the two oxides.

5. Conclusions

The interaction of CO with $CuO–CeO_2$, CuO and CuO/Al_2O_3 catalysts can be described as a reactive adsorption leading to surface reduction and formation of carbonates and concomitant reversible adsorption of CO on reduced sites (Cu^+). Reversibly adsorbed CO is weakly bound and desorbs with peak below 100 °C, but is highly reactive towards gaseous oxygen. Surface carbonates, formed by the interaction of CO with the catalysts at room temperature, decompose during TPD towards CO_2. The corresponding CO_2 profiles consist of a LT peak at 100–150 °C – common on all catalysts – along with CO_2 desorption at high temperatures in the case of $CuO–CeO_2$ catalysts activated at low temperature. Increase of catalyst activation temperature leads to CuO cluster growth and decrease of CO adsorption capacity, but this is not detrimental to catalyst activity, because the 'lost' sites are those which bind carbonate species and are inactive under reaction conditions. The beneficial effect of CeO_2 on the activity of $CuO–CeO_2$ catalysts may be attributed to the stabilization of highly dispersed CuO species with concomitant creation of additional CO adsorption and reaction sites, probably at the interface between the two oxides.

References

[1] G. Avgouropoulos, T. Ioannides, Appl. Catal. B: Environ. 67 (2006) 1.
[2] J.B. Wang, D.H. Tsai, T.J. Huang, J. Catal. 208 (2002) 370.
[3] D. Gamarra, G. Munuera, A.B. Hungria, M. Fernandez-Garcia, J.C. Conesa, P.A. Midgley, X.Q. Wang, J.C. Hanson, J.A. Rodriguez, A. Martinez-Arias, J. Phys. Chem. C 111 (2007) 11026.
[4] A. Martinez-Arias, M. Fernandez-Garcia, O. Galvez, J.M. Coronado, J.A. Anderson, J.C. Conesa, J. Soria, G. Munuera, J. Catal. 195 (2000) 207.
[5] G. Avgouropoulos, T. Ioannides, H. Matralis, J. Batista, S. Hocevar, Catal. Lett. 73 (2001) 33.
[6] G. Avgouropoulos, T. Ioannides, Appl. Catal. A: Gen. 244 (2003) 155.
[7] C.M. Bae, J.B. Ko, D.H. Kim, Catal. Commun. 6 (2005) 507.
[8] D.H. Tsai, T.J. Huang, Appl. Catal. A: Gen. 223 (2002) 1.
[9] W. Liu, M. Flytzani-Stephanopoulos, J. Catal. 153 (1995) 304.
[10] W. Liu, M. Flytzani-Stephanopoulos, Chem. Eng. J. 64 (1996) 283.
[11] A. Tchope, W. Liu, M. Flytzani-Stephanopoulos, J.Y. Ying, J. Catal. 157 (1995) 42.
[12] S.M. Zhang, W.P. Huang, X.H. Qiu, B.Q. Li, X.C. Zheng, S.H. Wu, Catal. Lett. 80 (2002) 41.
[13] J. Xiaoyuan, L. Guanglie, Z. Renxian, M. Jianxin, C. Yu, Z. Xiaoming, Appl. Surf. Sci. 173 (2001) 208.
[14] M.F. Luo, Y.J. Zhong, X.X. Yuan, X.M. Zheng, Appl. Catal. A: Gen. 162 (1997) 121.
[15] G. Avgouropoulos, T. Ioannides, H. Matralis, Appl. Catal. B: Environ. 56 (2005) 87.
[16] P.G. Harrison, I.K. Ball, W. Azelee, W. Daniell, D. Goldfarb, Chem. Mater. 12 (2000) 3715.
[17] F. Marino, B. Schonbrod, M. Moreno, M. Jobbagy, G. Baronetti, M. Laborde, Catal. Today 133–135 (2008) 735.
[18] D. Gamarra, C. Belver, M. Fernandez-Garcia, A. Martinez-Arias, J. Am. Chem. Soc. 129 (2007) 12064.
[19] P.A. Dilara, J.M. Vohs, J. Phys. Chem. 97 (1993) 12919.
[20] Y. Li, Q. Fu, M. Flytzani-Stephanopoulos, Appl. Catal. B: Environ. 27 (2000) 179.
[21] S. Hocevar, U.O. Krasovec, B. Orel, A.S. Arico, H. Kim, Appl. Catal. B: Environ. 28 (2000) 113.
[22] Lj. Kundakovic, M. Flytzani-Stephanopoulos, Appl. Catal. A: Gen. 171 (1998) 13.
[23] Y. Liu, T. Hayakawa, K. Suzuki, S. Hamakawa, Catal. Commun. 2 (2001) 195.
[24] A. Martinez-Arias, M. Fernandez-Garcia, J. Soria, J.C. Conesa, J. Catal. 182 (1999) 367.
[25] J.B. Wang, S.C. Lin, T.J. Huang, Appl. Catal. A: Gen. 232 (2002) 107.
[26] A. Tscope, M.L. Trudeau, J.Y. Ying, J. Phys. Chem. B 103 (1999) 8858.
[27] G. Sedmak, S. Hocevar, J. Levec, J. Catal. 213 (2003) 135.
[28] M. Luo, J. Ma, J. Lu, Y. Song, Y. Wang, J. Catal. 246 (2007) 52.
[29] J. Zhu, Q. Gao, Z. Chen, Appl. Catal. B: Environ. 81 (2008) 236.
[30] P. Bera, S.T. Aruna, K.C. Patil, M.S. Hegde, J. Catal. 186 (1999) 36.
[31] P. Bera, K.R. Priolkar, P.R. Sarode, M.S. Hegde, S. Emura, R. Kumashiro, N.P. Lalla, Chem. Mater. 14 (2002) 3591.
[32] G. Avgouropoulos, T. Ioannides, Catal. Lett. 116 (2007) 15.
[33] T. Caputo, L. Risi, R. Pirone, G. Russo, Appl. Catal. A 348 (2008) 42.
[34] C.R. Jung, J. Han, S.W. Nam, T. Lim, S. Hong, H. Lee, Catal. Today 93–95 (2004) 183.
[35] E. Giamello, B. Fubini, V. Bolis, Appl. Catal. A: Gen. 36 (1988) 287.
[36] H. Zou, X. Dong, W. Lin, Appl. Surf. Sci. 253 (2006) 2893.
[37] F. Bozon-Verduraz, A.A. Bensalem, J. Chem. Soc. Faraday Trans. 90 (1994) 653.
[38] C. Li, Y. Sakata, T. Arai, K. Domen, K. Maruya, T. Onishi, J. Chem. Soc. Faraday Trans. 85 (1989) 929.
[39] S. Hilaire, X. Wang, T. Luo, R.J. Gorte, J. Wagner, Appl. Catal. A: Gen. 215 (2001) 271.
[40] A. Karpenko, R. Leppelt, J. Cai, V. Plzak, A. Chuvilin, U. Kaiser, R.J. Behm, J. Catal. 250 (2007) 139.